



Comparative studies on impact of synthesis methods on structural and magnetic properties of magnesium ferrite nanoparticles

Navneet Kaur, Manpreet Kaur*

Department of Chemistry, Punjab Agricultural University, Ludhiana-141004, India

Received 12 August 2014; Received in revised form 24 September 2014; Accepted 27 September 2014

Abstract

Magnesium ferrite nanoparticles (NPs) were synthesized by co-precipitation, sol-gel and solution combustion methods. Polyethylene glycol (PEG), urea and oxalyl dihydrazide (ODH) were used as fuels for the combustion. Various physicochemical techniques viz. X-ray diffraction (XRD), vibrating sample magnetometry (VSM), Fourier transform infrared spectroscopy (FT-IR), BET surface analysis and transmission electron microscopy (TEM) were utilized to study the effect of synthetic methodology on the properties of synthesized NPs. Differences in crystallinity, surface area, particle size and magnetic parameters of the ferrite NPs synthesized by different methods were observed. XRD pattern of NPs obtained by sol-gel and combustion methods confirmed phase purity whereas in co-precipitation method α - Fe_2O_3 was detected as impurity phase which also resulted in greater value of physical density and lowering of magnetic parameters of the final thermolysis product. TEM micrographs indicated that ferrite NPs are spherical with average diameter of 12–25 nm. Presence of rectangular shaped crystallites of α - Fe_2O_3 was clearly evident in the TEM images of the NPs synthesized by co-precipitation method.

Keywords: Nano ferrite, combustion, co-precipitation, magnetic properties, calcination, structural properties

I. Introduction

Nanomaterials play a pivotal role in physical, chemical and biomedical fields due to their high surface energies. Among these, spinel ferrites are useful magnetic materials because of their low cost and high electromagnetic performance over a wide frequency range as compared to the pure metals [1]. Spinel ferrites are the compounds having a general formula AB_2O_4 , in which the A-site is tetrahedrally coordinated and occupied by divalent cations and the B-site is octahedrally coordinated and occupied by trivalent ion Fe^{3+} [2]. High resistivity of ferrites greatly influences their dielectric and magnetic behaviour [3]. They are widely used in electronic and magnetic devices due to their high magnetic permeability and low magnetic losses [4]. In the recent years, ferrite nanoparticles have received applications in the diverse fields such as mineral separation, magnetic storage devices [5], catalysis [6], magnetic refrigeration system, drug delivery system [7], magnetic resonance imaging [8], cancer therapy [9] and magnetic cell separation [10].

Magnesium ferrite is an important spinel ferrite which finds applications in the fields of heterogeneous catalysis, adsorption, sensors and magnetic technologies [11]. Several methods are employed to synthesize ferrite nanoparticles. Ceramic method is economical for the bulk synthesis of ferrites but undesired non-uniform particles are formed due to aggregation of nanoparticles and phase purity is not completely achieved. High-energy milling can reduce the crystallite size but this physical process not only requires greater energy consumption but also easily induces structural disorder in the crystallites [12]. In the recent past several chemical methods viz. co-precipitation [13], sol-gel [14], combustion [15], micelle routes [3] and hydrothermal synthesis [16] have been employed to synthesize ferrite nanoparticles under moderate conditions. NPs synthesized by these methods possess good chemical homogeneity and high purity [17].

Studies pertaining to the effect of synthetic method on the properties of ferrites are important in understanding their inter relationship and need to be explored. Properties of ferrite materials are strongly influenced by the distribution of metallic ions among crystallographic lattice sites which in turn is sensitive to the synthetic

*Corresponding author: tel: +91 814 6200711
e-mail: manpreetchem@pau.edu

method employed. Selection of the method largely depends on the targeted applications and desired properties. Although magnesium ferrite NPs have been synthesized by different chemical methods under different temperature and sintering conditions, comparative evaluation of effect of different synthetic methodologies on structural and magnetic properties of magnesium ferrite NPs at constant calcination temperature and sintering time are lacking. The objective of the present work is to assess the effect of these parameters on the structural and magnetic properties of spinel magnesium ferrite NPs prepared by different chemical routes viz. the sol-gel, co-precipitation and combustion methods.

II. Experimental

MgFe₂O₄ NPs were synthesized employing three different synthetic routes i.e. sol-gel, co-precipitation and combustion methods. All the chemicals used were of AR grade and all the solutions were prepared in double distilled water.

2.1. Sol-gel method

In the sol-gel method 2.0 mol of Fe(NO₃)₃·9H₂O and 1.0 mol of Mg(NO₃)₂·6H₂O were dissolved in 20 ml distilled water. Then 2.22 mol of citric acid was added in the aqueous mixture [18]. The mixture was magnetically stirred at 60 °C and ammonium hydroxide was added into the mixture to adjust solution pH to 7.0 and the mixture transformed into sol. After stirring for 8 h, the sol turned into gel. The gel was dried at 100 °C for 12 h with its volume expanding about five times. Finally, the dried gel was ground and calcined at 500 °C for 3 h to get ferrite as final thermolysis product.

2.2. Co-precipitation method

2.0 mol of Fe(NO₃)₃·9H₂O and 1.0 mol of Mg(NO₃)₂·6H₂O were dissolved in 20 ml distilled water. The pH of the solution was adjusted between 9 and 10 with 0.1 M NaOH resulting in the brown precipitates. The precipitates were filtered and washed repeatedly with distilled water till pH 7 was achieved. Finally, the precipitates were dried at 100 °C for 4 h and subsequently calcined at 500 °C for 3 h to get ferrite as end product.

2.3. Combustion method

Three different complexing agents/fuels, i.e. polyethylene glycol (PEG), urea and oxalyl dihydrazide (ODH), were used to prepare MgFe₂O₄ NPs by combustion method. ODH required for the synthesis was prepared using hydrazine hydrate and diethyl oxalate [19]. Metal nitrates act as oxidizers (*O*) and PEG/Urea/ODH act as fuel (*F*). Equivalence ratio i.e. $\phi_e = (O/F)$ was maintained unity by balancing the oxidizing (*O*) and reducing valency (*F*) of the reactants [20].

2.4. Characterization techniques

FT-IR spectra were recorded on Perkin Elmer, model RX-1 FT-IR spectrophotometer. The X-ray diffraction measurements were carried out using Cu K α radiation ($\lambda = 1.5404 \text{ \AA}$) with the Panalytical X'pert Pro. Magnetic properties of ferrite samples were studied by vibrating sample magnetometer model PAR-155. Transmission electron micrographs (TEM) of end products were recorded by employing transmission electron microscope model Hitachi Hi-7650 at 100 kV acceleration voltages in HC mode using water as a dispersion medium. The lattice constant, or lattice parameter (*a*) was calculated employing the following relationship:

$$a = d(h^2 + k^2 + l^2)^{1/2} \quad (1)$$

where *d* is diffracting plane spacing and *h*, *k* and *l* Miller indices of the diffracting plane.

The XRD density (ρ_{XRD}) was calculated by the formula:

$$\rho_{XRD} = \frac{8M}{N a^3} \quad (2)$$

where, *M* is molecular weight of the sample and *N* is Avogadro's number.

The crystallite size of the MgFe₂O₄ NPs was based on X-ray diffraction line broadening and calculated by using Scherrer's equation [21]:

$$D = \frac{B\lambda}{\beta \cos \theta} \quad (3)$$

where *D* is the average crystallite size of the phase under investigation, *B* is the Scherrer's constant (0.89), λ is the wave length of X-ray beam used, β is the full-width half maximum of diffraction peak and θ is the Bragg's angle.

III. Results and discussion

3.1. FT-IR parameters

FT-IR spectrum of ferrite NPs obtained using polyethylene glycol as fuel is shown in Fig. 1. The spectrum displayed two bands in the region 400–630 cm⁻¹. The higher frequency band (ν_1) located in the region 520–630 cm⁻¹ corresponds to stretching vibrations of metal ions in the tetrahedral sites and some additional peaks observed in the region above 630 cm⁻¹ were due to the splitting of absorption band due to exchange of ions between A and B sites. Similar results have been reported earlier [22]. The second lower frequency band (ν_2) observed in the region 400–482 cm⁻¹ was due to the stretching vibrations of metal ions in the octahedral site [23]. The difference in band position was caused by difference in M–O distance in tetrahedral and octahedral sites [24]. Magnesium ferrite synthesized by other methods also displayed similar absorption bands.

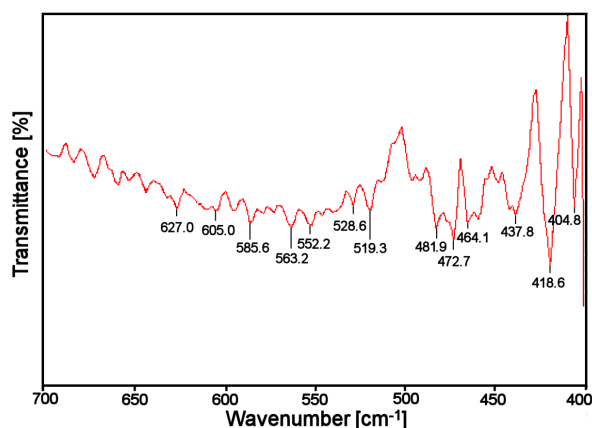


Figure 1. FT-IR spectrum of MgFe_2O_4 NPs synthesized by PEG-metal nitrate combustion method

3.2. XRD parameters

X-ray diffractograms of MgFe_2O_4 NPs synthesized by different chemical methods are shown in Fig. 2 and XRD parameters are given in Table 1. The diffraction patterns of MgFe_2O_4 consisted of peaks corresponding to crystallographic planes (220), (311), (400), (422), (511) and (440). All the observed peaks and Miller indices (hkl) of the fcc lattice were in agreement with the reported values [25,26] for MgFe_2O_4 and also confirmed by matching with ASTM Data Card No. 17-465. The peak broadening of the diffraction patterns is mainly attributed to four factors: faulting (extended defects), micro strains (deformation of the lattice) and crystalline domain size distribution. If the samples are free from strains and faulting, the peak broadening is

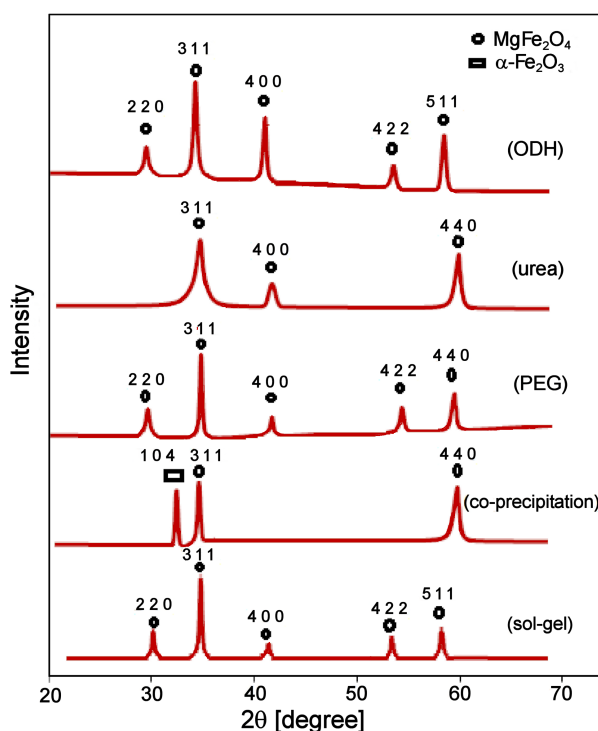


Figure 2. X-ray diffraction patterns of MgFe_2O_4 synthesized by different chemical routes

only due to the crystalline domain size [27]. The crystallite size of the samples prepared by different methods was in the range of 8–16 nm respectively. The difference in crystallite size was due to different preparation conditions for ferrite synthesis. NPs synthesized by the sol-gel method (Fig. 2) displayed the most intense XRD peaks, indicating their highest crystallinity among the synthesized NPs. Lattice constant obtained using the XRD data is found to be in the range 8.308 Å to 8.351 Å. X-ray diffractogram of NPs obtained by the chemical co-precipitation method (Fig. 2) displayed weak diffraction peaks corresponding to $\alpha\text{-Fe}_2\text{O}_3$ along with sharp peaks for spinel ferrite component due to the low crystallinity, which indicates that in co-precipitation method phase purity is not completely achieved. Fe_2O_3 impurity phase was previously reported in MgFe_2O_4 NPs synthesized by co-precipitation method [28] and it is clearly evident that the phase purity is determined by preparation method. Physical density of sol gel, co-precipitation and combustion derived NPs are shown in Table 1. Ferrite NPs synthesized by combustion and sol-gel methods displayed lower values than the corresponding XRD density which was expected due to the presence of pores created in the powders during the sintering process, whereas greater value of physical density of ferrites synthesized by co-precipitation method and their non-porous nature can be attributed to the presence of $\alpha\text{-Fe}_2\text{O}_3$ impurity. It has been reported that the density of bioactive glass-ceramics increased with increase in Fe_2O_3 content [29], moreover Fe_2O_3 containing samples have improved hydration resistance due to their larger grain size compared to Fe_2O_3 free samples [30].

3.3. Magnetic studies

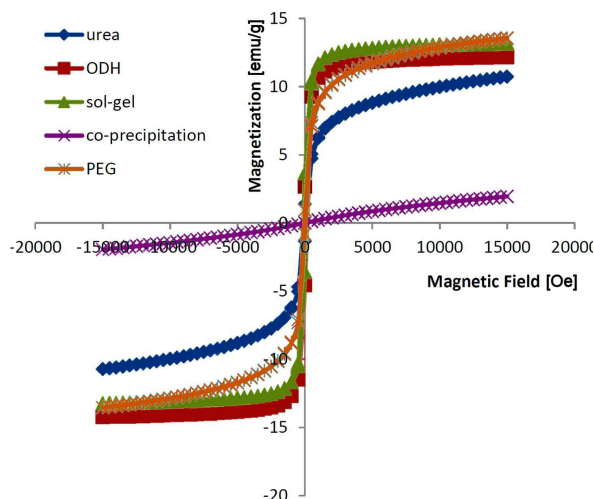
Hysteresis plots showing the variation of magnetization (M_s , emu/g) as a function of applied magnetic field (H , Oe) are shown in Fig. 3 and magnetic parameters are presented in Table 2. All the samples displayed normal (S-shaped) narrow hysteresis loops. Narrow loop indicated low coercivity values which indicate that the prepared sample can be easily demagnetized. Magnetic parameters like saturation magnetization (M_s), remnant magnetization (M_r) and coercivity (H_c) of the samples depend upon a number of factors viz. anisotropy density, grain growth and A–B exchange interactions. M_s values of NPs synthesized by PEG, sol-gel, ODH and urea combustion methods were 13.55, 13.22, 13.25 and 10.73 emu/g, respectively. Although urea has greater combustion heat (–2.98 kcal/g) as compared to citric acid (–2.76 kcal/g) [31] the observed M_s has higher value for the later. This could be explained on the basis of better complexation power of the citric acid and greater amount of heat evolved when equimolar amount of citric acid is used. Polymerization is favoured upon heating and the resultant citrate gel is a polymeric network with metal ions uniformly distributed throughout the organic matrix. Autocatalytic combustion of polymeric gel and polyethylene glycol also favours greater

Table 1. XRD parameters of ferrite nanoparticles

Method	Lattice constant [Å]	X-Ray density [g/cm ³]	Physical density [g/cm ³]	Porosity [%]	Average particle diameter [nm]
Sol-gel	8.351	3.819	2.586	32.28	16.0
Co-precipitation	8.321	3.837	5.431	-	13.5
PEG	8.314	3.843	3.235	15.82	16.0
Urea	8.312	3.844	3.017	21.51	8.0
ODH	8.308	3.848	1.852	51.87	11.0

Table 2. Magnetic parameters of ferrite nanoparticles synthesized by different chemical methods

Method	Saturation magnetization, M_s [emu/g]	Retentivity, M_r [emu/g]	Coercivity, H_c [Oe]
Sol gel	13.22	3.62	130.55
Co precipitation	1.95	-	2.59
PEG	13.55	0.89	55.47
Urea	10.73	1.36	112.02
ODH	13.25	3.45	66.05

**Figure 3. Hysteresis loop of MgFe₂O₄ synthesized by different chemical methods**

crystallinity for NPs synthesized by these methods. NPs prepared by co-precipitation method had lowest M_s value of 1.948 emu/g. Presence of ferric oxide phase along with ferrite phase due to incomplete precipitation resulted in the observed decline in magnetic behavior. Another possible reason for the diminution in the value of M_s may be attributed to the incomplete crystallization of MgFe₂O₄ which is undetectable by XRD technique. The higher saturation values for NPs obtained from the PEG, sol-gel and ODH methods may be due to the fact that the anisotropic features of these nanocrystals have enhanced dipole-dipole interaction, favouring a head-to-tail orientation [32]. The second factor favouring increase in the value of M_s and M_r for sol-gel and PEG synthesized NPs is the increase in crystalline size. It was also observed that MgFe₂O₄ NPs prepared by combustion method at calcination temperature 900 °C had a crystalline size of 78.8 nm and M_s value of 30.6 emu/g [33]. H_c of the magnetic material

is a measure of its magneto-crystalline anisotropy. The values of H_c have no direct relationship with the preparation temperature and/or crystalline size. These values are altered by M_r values. Higher remanent magnetization favours increase in coercive field. NPs synthesized by PEG method displayed high M_s values coupled with low coercivity which is an essential requirement for a good electromagnet. The lower values of magnetic parameters as compared to bulk counterparts are attributed to the smaller particle size of the ferrite NPs [34] and existence of spin canting, which has been reported in several nanometer-sized ferrites and is dependent upon surface structural disorder [35].

3.4. TEM and BET studies

Particle morphology and size distribution of the ferrite powder calcined at 500 °C were investigated using TEM micrographs. Figure 4 displays the TEM micrographs and particle size distribution histograms of the NPs synthesized by sol-gel, co-precipitation and combustion methods. NPs synthesized by sol-gel method (Fig. 4a) show average particle diameter of 25 nm and these results are corroborated with the XRD results where sharp peaks confirmed greater crystallinity.

In case of co-precipitation derived ferrites (Fig. 4b) the particle size distribution displayed large variation and rectangular shaped α -Fe₂O₃ particles (as depicted by arrow) are clearly visible in the TEM micrograph. Average particle diameter of ferrite NPs was 12 nm. Similar results were reported in case of nickel ferrite synthesized by co-precipitation method [36].

TEM micrographs of ferrite NPs synthesized by combustion methods (Figs. 4c,d) confirm nanocrystalline nature of combustion derived ferrite NPs with average particle diameter of 14.5 and 17.3 nm respectively for PEG and ODH derived NPs. Spherical shape of the NPs was clearly visible and impurity phase was not detected in sol-gel and combustion derived NPs. Agglomeration

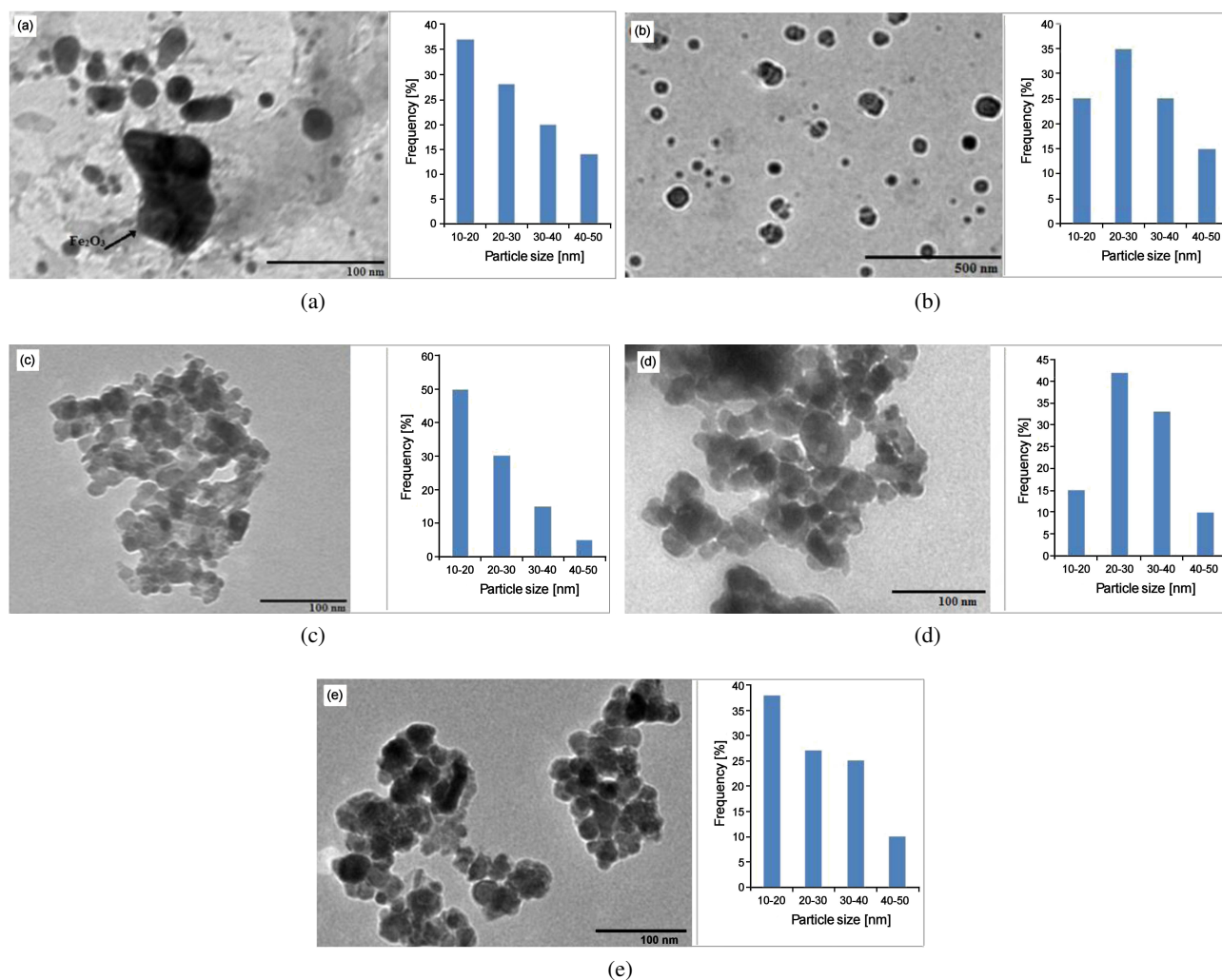


Figure 4. Transmission electron micrographs and particle size distribution histograms of calcined MgFe_2O_4 synthesized by: a) co-precipitation method, b) sol-gel method, c) PEG method and d) Urea method and e) ODH method

phenomenon was also observed as small particles aggregated in order to achieve lower free energy state. NPs synthesized using urea as a fuel (Fig. 4e) showed greater agglomeration of the primary particles and average size of 21 nm. This trend was also observed by Wu *et al.* [37] during synthesis of SiO_2 doped Ni-Zn ferrites by using different fuels. TEM images of these NPs clearly reveal self alignment of NPs. The particle size estimated from TEM was greater than the particle size calculated from XRD using Scherrer's formula. This is because X-ray diffraction gives the information of the crystalline region only and the contribution from the amorphous grain surface does not contribute. On the other hand TEM images display the complete morphology of the nanoparticles. MgFe_2O_4 NPs synthesized by sol-gel, co-precipitation, PEG and urea method displayed BET surface area of 3.8, 67.2, 17.1 and 27.5 and $26.5 \text{ m}^2/\text{g}$, respectively. The large surface area of co-precipitation derived ferrites was due to hindrance in the growth of particles due to incomplete ferritization and presence of $\alpha\text{-Fe}_2\text{O}_3$ in the final thermolysis product. The results of BET surface area study were in

accordance with the observed average particle size trend of the TEM studies.

IV. Conclusions

MgFe_2O_4 NPs are synthesized by sol-gel, co-precipitation and combustion methods keeping uniform calcination temperature and sintering time. Differences in crystallinity, surface area, particle size and magnetic parameters of the ferrite NPs synthesized by different methods were observed. TEM micrographs showed that NPs exhibited agglomeration phenomenon and had an average diameter of 12–25 nm. Rectangular shaped nanocrystals of $\alpha\text{-Fe}_2\text{O}_3$ were observed in the TEM images of NPs synthesized by co-precipitation method which was confirmed by the XRD pattern. Magnesium ferrite synthesized PEG, ODH and sol-gel methods displayed M_s values ranging from 13.22–13.55 emu/g whereas NPs synthesized by urea method had lower M_s value of 10.73 emu/g which was in accordance with the observed lower crystallinity. The lowest value of M_s 1.95 emu/g for NPs synthesized by co-precipitation

method confirmed the effect of impurity phase on the diminution of magnetic parameters.

Acknowledgment: Manpreet Kaur acknowledges the financial assistance (grant number 42-337/2013) provided by University Grants Commission, India.

References

- G. Dixit, J.P. Singh, R.C. Srivastava, H.M. Agarwal, R.J. Chaudhary, "Structural, magnetic and optical studies of nickel ferrite thin films", *Adv. Mater. Lett.*, **3** [1] (2012) 21–26.
- B. Viswanathan, V.R.K. Murthy, *Ferrite Materials*, Narosa Publishers, New Delhi, 1990.
- T. Ahmad, K.V. Ramanujachary, S.E. Lofland, A.K. Ganguli, "Reverse micellar synthesis and properties of nanocrystalline GMR materials (LaMnO_3 , $\text{La}_{0.67}\text{Sr}_{0.33}\text{MnO}_3$ and $\text{La}_{0.67}\text{Ca}_{0.33}\text{MnO}_3$): Ramifications of size considerations", *J. Chem. Sci.*, **118** [6] (2006) 513–518.
- W. Yan, Q. Li, H. Zhong, Z. Zhong, "Characterization and low-temperature sintering of $\text{Ni}_{0.5}\text{Zn}_{0.5}\text{Fe}_2\text{O}_4$ nano-powders prepared by refluxing method", *Powder Technol.*, **192** (2009) 23–26.
- V.G. Harris, A. Geiler, Y. Chen, "Recent advances in processing and applications of microwave ferrites", *J. Magn. Magn. Mater.*, **321** (2009) 2035–2047.
- Y. Qu, H. Yang, N. Yang, "The effect of reaction temperature on the particle size, structure and magnetic properties of coprecipitated CoFe_2O_4 nanoparticles", *Mater. Lett.*, **60** (2006) 3548–3552.
- N. Kasapoglu, B. Birsoz, A. Baykal, "Synthesis and magnetic properties of octahedral ferrite $\text{Ni}_x\text{Co}_{1-x}\text{Fe}_2\text{O}_4$ nanocrystals", *Cent. Eur. J. Chem.*, **5** (2007) 570–580.
- S.W. Cao, Y.J. Zhu, G.F. Cheng, "Zn Fe_2O_4 nanoparticles: Microwave-hydrothermal ionic liquid synthesis and photocatalytic property over phenol", *J. Hazard. Mater.*, **171** (2009) 431–435.
- Y.L. Liu, Z.M. Liu, Y. Yang, "Simple synthesis of MgFe_2O_4 nanoparticles as gas sensing materials", *Sensor. Actuat. B-Chem.*, **107** (2005) 600–604.
- M. Koledintseva, J. Drewniak, Y. Zhang, J. Lenn, M. Thoms, "Modeling of ferrite-based materials for shielding enclosures", *J. Magn. Magn. Mater.*, **321** (2009) 730–733.
- S.V. Bangale, D.R. Patil, S.R. Bamane, "Preparation and electrical properties of nanocrystalline MgFe_2O_4 oxide by combustion route", *Arch. Appl. Sci. Res.*, **3** [5] (2011) 506–513.
- S.K. Pradhan, S. Bid, M. Gateshki, V. Petkov, "Microstructure characterization and cation distribution of nanocrystalline magnesium ferrite prepared by ball milling", *Mater. Chem. Phys.*, **93** (2005) 224–230.
- N.D. Kandpal, N. Sah, R. Loshali, R. Joshi, J. Prasad, "Co-precipitation method of synthesis and characterization of iron oxide nanoparticle", *J. Sci. Ind. Res.*, **73** (2014) 87–90.
- M. Kaur, B.S. Randhawa, P.S. Tarsikka, "Synthesis of $\text{Mg}_{0.3}\text{Zn}_{0.7}\text{Fe}_2\text{O}_4$ nanoparticles from thermolysis of magnesium zinc tris maleatoferrate (III) heptahydrate", *Ind. J. Eng. Mater. Sci.*, **20** (2013) 325–328.
- M. Kaur, S. Rana, P.S. Tarsikka, "Comparative analysis of cadmium doped magnesium ferrite $\text{Mg}_{(1-x)}\text{Cd}_x\text{Fe}_2\text{O}_4$ ($x = 0.0, 0.2, 0.4, 0.6$) nanoparticles", *Ceram. Int.*, **38** (2012) 4319–4323.
- W.L. Suchanek, R.E. Riman, "Hydrothermal synthesis of advanced ceramic powders", *Adv. Sci. Technol.*, **45** (2006) 184–193.
- K.S. Yang, H.O. In, "Preparation of ultrafine $\text{YBa}_2\text{Cu}_3\text{O}_{7-x}$ superconductor powders by the Poly(vinyl alcohol)-Assisted sol-gel method", *Ind. Eng. Chem. Res.*, **35** (1996) 4296–4300.
- C.P. Liu, M.W. Li, Z. Cui, J.R. Huang, Y.L. Tian, T. Lin, W.B. Mi, "Comparative study of magnesium ferrite nanocrystallites prepared by sol-gel and coprecipitation methods", *J. Mater. Sci.*, **42** (2007) 6133–6138.
- B.S. Randhawa, H.G. Dosanjh, M. Kaur, "Preparation of ferrites from the combustion of metal nitrate-oxalyl dihydrazide solutions", *Ind. J. Eng. Mater. Sci.*, **12** (2005) 151–154.
- T. Mimani, "Fire synthesis-preparation of alumina products", *Reson.*, **16** (2011) 1327.
- B.D. Cullity, *Elements of X-ray Diffraction*, Addison-Wesley Publishing Co. Inc. 1976 (Chapter 14).
- V.A. Potakova, N.D. Zverev, V.P. Romanov, "On the cation distribution in $\text{Ni}_{1-x-y}\text{Fe}_x^{2+}\text{Zn}_y\text{Fe}_2^{3+}\text{O}_4$ spinel ferrites", *Phys. Status Solidi A*, **12** [2] (1972) 623–627.
- K. Nakamoto, *Infrared Spectra of Inorganic and Coordination Compounds* (John Wiley Intersci, New York), 1970.
- M.Z. Khan, M.U. Islam, M. Ishaque, I.Z. Rahman, "Effect of Tb substitution on structural, magnetic and electrical properties of magnesium ferrites", *Ceram. Int.*, **37** (2011) 2519–2526.
- R. Arulmurugan, B. Jeyadevan, G. Vaidyanathan, S. Sendhilnathan, "Effect of zinc substitution on Co-Zn and Mn-Zn ferrite nanoparticles prepared by coprecipitation", *J. Magn. Magn. Mater.*, **288** (2005) 470–477.
- H. Spiers, I.P. Parkin, Q.A. Pankhurst, L. Affleck, M. Green, D.J. Caruana, M.V. Kuznetsov, J. Yao, G. Vaughan, A. Terry, A. Kvick, "Self propagating high temperature synthesis of magnesium zinc ferrites $\text{Mg}_x\text{Zn}_{1-x}\text{Fe}_2\text{O}_4$: Thermal imaging and time resolved X-ray diffraction experiments", *J. Mater. Chem.*, **14** (2004) 1104–1111.
- Y.S. Fu, X.W. Du, A. Sergai, J. Liu, "Influence of processing methodology on the structural and magnetic behavior of MgFe_2O_4 nanopowders", *J. Am.*

- Chem. Soc.*, **129** (2007) 16029–16035.
28. C.P. Liu, M.W. Li, Z. Cui, J.R. Huang, Y.L. Tian, T. Lin, W.B. Mi, “Comparative study of magnesium ferrite nanocrystallites prepared by sol-gel and coprecipitation methods”, *J. Mater. Sci.*, **42** (2007) 6133–6138.
29. A.K. Srivastava, R. Pyare, S.P. Singh, “In vitro bioactivity and physical-mechanical properties of Fe₂O₃ substituted 45S5 bioactive glasses and glass-ceramics”, *Int. J. Sci. Engg. Res.*, **3** (2012) 89–103.
30. A. Ghosh, T.K. Bhattacharya, B. Mukherjee, H.S. Tripathi, S.K. Das, “Effect of Fe₂O₃ on the densification and properties of lime”, *Ceram. Silikaty*, **47** (2003) 70–74.
31. A.B. Salunkhe, V.M. Khot, M.R. Phadatare, “Combustion synthesis of cobalt ferrite nanoparticles- Influence of fuel to oxidizer ratio”, *J. Alloys Compd.*, **514** (2012) 91–96.
32. D. Yu, X. Sun, J. Zou, Z. Wang, F. Wang, K.J. Tang, “Oriented assembly of Fe₃O₄ nanoparticles into monodisperse hollow single-crystal microspheres”, *J. Phys. Chem. B.*, **110** [43] (2006) 21667–21671.
33. Y. Huang, Y. Tang, J. Wang, Q. Chen, “Synthesis of MgFe₂O₄ nanocrystallites under mild conditions”, *Mater. Chem. Phys.*, **97** (2006) 394–397.
34. A. Pradeep, P. Priyadharsini, G. Chandrasekaran, “Sol-gel route of synthesis of nanoparticles of MgFe₂O₄ and XRD, FTIR and VSM study”, *J. Magn. Magn. Mater.*, **320** (2008) 2774–2779.
35. M.M. Rashad, “Magnetic properties of nanocrystalline magnesium ferrite by co-precipitation assisted with ultrasound irradiation”, *J. Mater. Sci.*, **42** (2007) 5248–5255.
36. B.P. Jacob, A. Kumar, R.P. Pant, S. Singh, E.M. Mohammed, “Influence of preparation method on structural and magnetic properties of nickel ferrite nanoparticles”, *Bull. Mater. Sci.*, **34** (2011) 1345–1350.
37. K.H. Wu, T.H. Ting, C.C. Yang, “Effect of complexant/fuel on the chemical and electromagnetic properties of SiO₂-doped Ni-Zn ferrite”, *Mater. Sci. Eng. B.*, **123** (2005) 227–233.

